Journal of Applied Polymer Science

Effects of TiO_2, ZnO, and Fe_3O_4 nanofillers on rheological behavior, microstructure, and reaction kinetics of rigid polyurethane foams

Meral Akkoyun, Ender Suvaci
Department of Materials Science and Engineering, Anadolu University, Iki Eylul Campus, Eskisehir 26480, Turkey
Correspondence to: M. Akkoyun (E-mail: meralakkoyun@anadolu.edu.tr)

ABSTRACT: Effects of different types and shapes of titanium dioxide, zinc oxide, and magnetite nanofillers on the rheological behavior of polyol/nanofiller suspensions, on the rigid polyurethane foam formation reaction, and hence on the final microstructure were investigated. The rheological percolation threshold of polyol/nanofiller suspensions decreased as the aspect ratio of nonspherical nanoparticles (platelet or rod) increased, regardless of the nanofiller type. The results of reaction kinetics showed that above a critical surface area (≈30 m^2), independently of nanofiller type, the reaction rate increased as the surface area increased. The introduction of oxide surfaces reduced the final cell size until a critical surface area (≈30 m^2). However, above this critical value cell size distribution gets wider and the cell size can no longer be correlated with the surface area. In the latter case, an increase of the reaction rate and the polymerization reaction being exothermic may facilitate uncontrolled cell nucleation, growth, and hence coalescence which results in an uncontrolled foam structure. © 2016 Wiley Periodicals, Inc. J. Appl. Polym. Sci. **2016**, *133*, 43658.

KEYWORDS: composites; foams; kinetics; polyurethanes; rheology

Received 15 July 2015; accepted 20 March 2016
DOI: 10.1002/app.43658

INTRODUCTION

Polyurethane is a preferred polymeric material for various applications such as automobile, furnishing, insulation, coatings, and adhesives due to its low manpower costs and ease of processing.[1] Polyurethanes can be used as solid foams which include rigid foams (closed cell) and flexible ones (open cell). Their preparation process can be separated into four main steps. The first step consists of the dispersion of chemical or physical foaming agents in the polymeric matrix, the physical ones being more appropriate and preferred because of the absence of hazardous chemical solvent use during the foaming process. The next steps are cell nucleation, cell growth, and stabilization of the foam microstructure. Polyurethane foams are prepared by adding a foaming gas in the mixture of polyol and isocyanate. For rigid foams, due to its more favorable physiological properties, methylene diphenyl diisocyanate (MDI) is the most commonly used isocyanate. Aromatic or aliphatic polyesters and polyethers are generally used as polyols. Polyurethane foam chemistry is based on the simultaneous and highly exothermic reactions of isocyanates with polyols and water (Figure 1). The nature of the components used (polyol, isocyanate, and additives) has significant effects on the final properties of the foams. In addition, the nature of the catalyst can also play a critical role on foam structure development and properties.[2] Waste polyurethane foams can be valorized by chemical recycling to obtain polyurethane elastomers.[2]

Polyurethane foams have better thermal and sound barrier properties than other common insulation materials[3] even though they exhibit relatively low mechanical strength and low thermal stability.[4,5] Furthermore, the microstructural characteristics of polyurethane foams such as cell density, cell size and size distribution control the final properties of the foams.[6] In this literature, most of the studies deal with the improvement of the mechanical and thermal properties of the foams. In this sense, fillers and particularly nanofillers are used to reinforce the polymer matrix. Besides, nanofillers act as heterogeneous nucleation sites and allow to decrease the cell size. In fact, in heterogeneous nucleation, the initial cell formation is supported by the presence of foreign surfaces (nanofillers) and a simultaneous growth of the cells is observed which allows a narrow cell size distribution.[7] As mentioned, in recent years, nanofillers were used to reduce the cell size of polyurethane foams[8–15] with a rising interest to nanocellular polymer nanocomposite foams.[16] Widya *et al.*[14] showed that the use of montmorillonite as nanofiller in polyurethane foams allowed to decrease the average cell size from 400 to 280 μm.

During foaming process, the use of nanofillers can affect both cell nucleation and cell growth. Because of their smaller size and

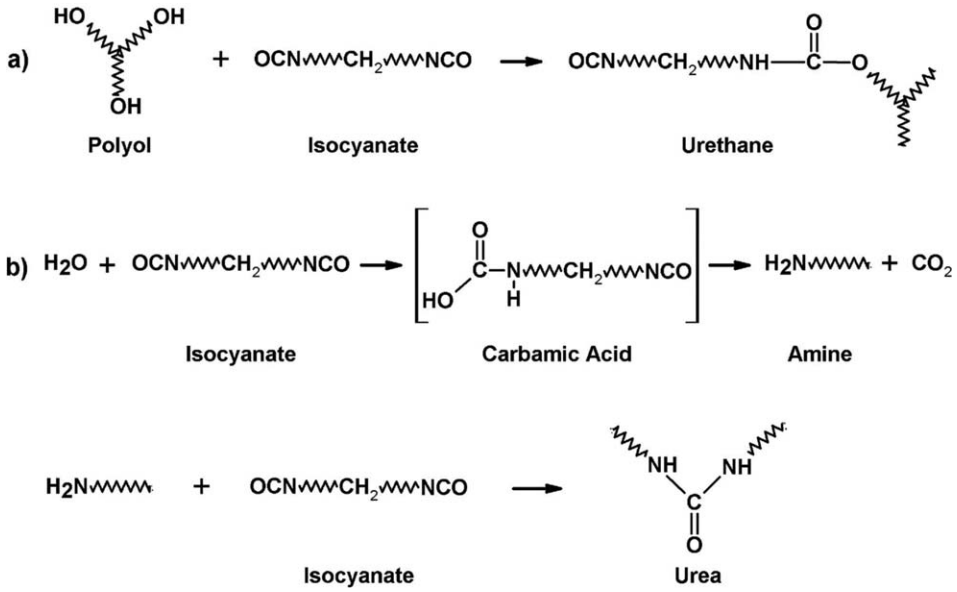

Figure 1. Chemistry of polyurethane foams: (a) Gelling reaction and (b) Blowing reaction.

hence their higher surface area compared to microscale fillers, for a given concentration, more nucleation sites can be introduced into the system.[7] Furthermore, the presence of nanofillers modifies the rheological properties of the reacting medium and increases the viscosity which prevents the cell growth during the foaming process and results in a decrease of the cell sizes.[17]

According to the literature, it is obvious that the properties of nanocomposites depend on the nanofillers type as well as their dispersion in the matrix.[18–22] Therefore, in the case of nanofilled polyurethane foams, the investigation of the dispersion of nanofillers in the polyol and/or the isocyanate is important. Rheological and physicochemical properties of the suspensions affect the properties of the foams. Very few studies exist on the rheological behavior of nanofiller/polyol or nanofiller/isocyanate suspensions and its effect on the final structure and properties of polyurethane foams. According to Harikrishnan *et al.*,[18] the microstructure and thermal conductivity properties of polyurethane foams are significantly affected by the rheological behavior of the suspensions (isocyanate/nanofiller). The rheological behavior of a polymer/filler system can be evaluated using the percolation theory.[19] When the degree of percolation is below the percolation threshold (φ_c), only a few number of links between particles are present in the system. When φ_c is reached, a continuous network is formed. Above φ_c, the number of bonds between the particles becomes important. Theoretical and experimental studies about the effect of the aspect ratio of nanofillers on the percolation threshold for polymer/carbon nanotubes[20,21] and polymer/graphite nanocomposites[22] are reported in the literature. Li *et al.*[21] theoretically investigated the effect of the filler dispersion and demonstrated an increase of the percolation threshold with the improvement of the dispersion parameters; such as the localized volume content of carbon nanotubes in an agglomerate, and the volume fraction of agglomerated carbon nanotubes.

Studies on polyurethane foams prepared with fillers as TiO_2,[6] Fe_3O_4,[23,24] SiO_2,[25] or clays[11–13] showed that the foam cell size was smaller compared to the corresponding neat polyurethane foam. The reduction of cell size was attributed to the possible effect of the nanofillers on the nucleation process. In recent years, *in situ* techniques have been developed to have a better understanding of the foaming mechanism of nano-reinforced thermoset polyurethane foams and to investigate the impact of nanofillers on the process. An example of that is the study of the foaming reaction kinetics using FTIR spectroscopy (attenuated total reflectance) with the monitoring of carbonyl and isocyanate functional group peaks.[26–29] Using this method, Bernal *et al.*[26] observed that the increase of carbon nanotubes (CNT) amount in polyurethane/CNT foams led to the decrease of isocyanate conversion rates. This observation has been referenced by several studies[27,30] showing that the high initial viscosity of the system induces a lower mobility of the molecules during the reaction.

Based on the literature, it can be concluded that the final properties of polyurethane/nanofiller nanocomposite foams depend on the microstructure, which is influenced by the type of the nanofillers and the matrix. In addition, the rheological properties of polymer/nanofiller suspensions have an important effect on the properties of polyurethane/nanofiller nanocomposite foams. Although these factors are important for the final microstructure of polyurethane foams, the effects of the aspect ratio and the nanofillers type on the percolation threshold were not studied for polyol/nanofiller systems. Furthermore, the effect of nanofillers type, shape, aspect ratio, and total surface area on the cell size of the different foams and on the foaming reaction kinetics still have to be investigated to develop a thorough understanding of polyurethane nanocomposites.

Thus, the objectives of this study were to understand: (i) the effect of the nanofillers type and shape on the rheological percolation threshold of the different polyol/nanofiller suspensions, (ii) the effect of nanofillers type, shape, concentration and surface area on the foaming reaction kinetics, and (iii) the effect of

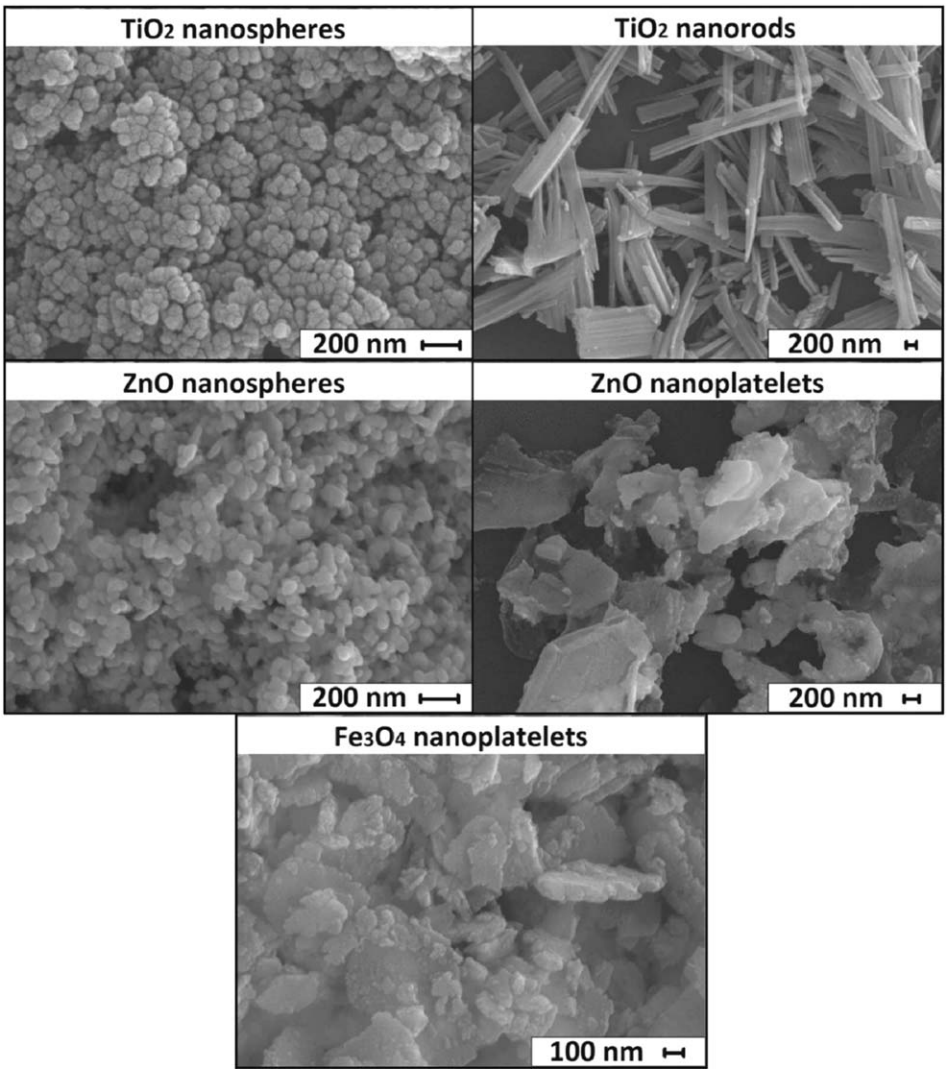

Figure 2. SEM micrographs of the nanofillers.

the nanofillers type, shape, concentration, and surface area on the foam morphology through the cell size evolution. A rheological study of the different polyol/nanofiller suspensions was conducted using nanofillers of different types, shapes and concentrations [titanium dioxide (TiO_2) nanospheres and nanorods, zinc oxide (ZnO) nanospheres, and nanoplatelets and magnetite (Fe_3O_4) nanoplatelets]. The percolation threshold of the suspensions was determined to understand and control the evolution of the systems and to identify the appropriate concentration range for the foam preparation. The viscosity of the different polyol/nanofiller suspensions was also monitored to determine its effect on the foaming process. Effects of different parameters on the reaction kinetics and on the microstructure of nanofilled rigid polyurethane foams were also investigated.

EXPERIMENTAL

Materials

Commercial grade isocyanate (VORATEC SD100) (NCO content of 31%, density of 1.23 g/cm^3 and viscosity of 0.2 Pa s), polyol (DSD459.01) (hydroxyl number of 386 mg KOH/g, density of 1.08 g/cm^3 and viscosity of 5.9 Pa s), and cyclopentane (70%) from Dow Chemical were used in this study. Five nanofillers with various types and shapes were selected: titanium dioxide (TiO_2) nanospheres and nanorods, zinc oxide (ZnO) nanospheres and nanoplatelets, and magnetite (Fe_3O_4) nanoplatelets. TiO_2 (≥99% purity) and ZnO (99% purity) nanospheres and Fe_3O_4 (95% purity) were from Sigma Aldrich, Alfa Aesar, and Komur İşletmeleri A.Ş. (KİAŞ/Turkey), respectively. TiO_2 (96% purity) nanorods and ZnO (97% purity) nanoplatelets were synthesized as described by Ozogut[31] and Yakaboylu[32] from Anadolu University and used directly. All materials were used as received.

Fe_3O_4 powder from KİAŞ/Turkey has an average initial particle size of about 70 μm. Due to its high initial particle size, the magnetite powder was first milled using a vibrating cup mill for 30 min for rapid reduction of the particle size. The particle size decreased from about 70 μm to about 3 μm. The second step was performed as described by Karunaratne *et al.*,[33] in which a planetary mill (Fritsch/Pulverisette6) was used, containing a silicon nitride bowl of 250 mL with 0.3 mm zirconia balls.

Table I. Characteristics of the Nanofillers

Nanofillers	Average diameter/ length (nm)	Average thickness (nm)[b]	Aspect ratio[b]	Average diameter (crystallite size)[c] (nm)	Specific surface area (m^2 g^{-1})[d]
TiO_2 nanospheres	<25[a]	-	1	17	39.3
TiO_2 nanorods	3701[b]	62	59.7	19	51.3
ZnO nanospheres	25–30[a]	-	1	27	31.6
ZnO nanoplatelets	1423[b]	50	28.4	30	19.9
Fe_3O_4 nanoplatelets	320[b]	35	9.1	20	32.3

[a] Suppliers' values.
[b] SEM.
[c] XRD.
[d] BET.

Magnetite from step-1 (25 g) was used in a liquid medium of 100 mL oleic acid (Merck). Milling was continued for 20 h until the desired particle size was obtained.

Figure 2 shows scanning electron microscope (SEM) micrographs of the nanofillers, obtained from a Zeiss Supra 50 V SEM at 20 kV and using a magnification range varying from 40 000× to 150,000×. Particle sizes of TiO_2 nanorods and nanospheres, ZnO nanoplatelets and nanospheres, and Fe_3O_4 nanoplatelets measured using various methods are presented in Table I. The aspect ratios related to these nanofillers are also shown in Table I. The average diameter/length and thickness of the different nanofillers were determined from at least 40 particles in SEM micrographs using Image J software. Furthermore, the specific surface areas of the nanofillers were obtained from Brunauer-Emmett-Teller (BET) analyses (Quantachrome Nova 2200e). Crystallite size of the fillers was determined from X-ray line broadening by using Scherrer's formula.

Foam Preparation

The nanofillers were first dried in an oven at 100 °C for 2 h and added in the polyol. The mixture was then sonicated using a Cole Parmer CP750 ultrasonic homogenizer for 2 min, to obtain a homogeneously dispersed suspension. For each nanofiller, rigid polyurethane foams were prepared at concentrations of 1 and 10 wt % in polyol. Nanofilled rigid polyurethane foams were prepared using a three-step procedure.[6] In addition to the effect of the types and shapes of the different nanofillers, the effect of the nanofillers concentration on the foaming reaction kinetics and on the foam morphology were also studied. Particle size measurements were performed for polyol/nanofiller suspensions at various sonication times from 1 to 5 min with the dynamic light scattering method to check the efficiency of the homogenization time and to determine whether the particles were agglomerated in the polyol. X-ray diffraction (XRD) measurements were also performed for the different nanofillers using a Rigaku Rint 2200 instrument.

The results obtained from dynamic light scattering measurements showed a decrease of the average particle size up to 2 min and then a stabilization was observed. The particle sizes obtained for each powder were consistent with the values given by the suppliers and those determined from XRD patterns. As a result, it was assumed that a homogenization time of 2 min allows a good dispersion of nanofillers in the polyol. Accordingly, during the preparation of nanofilled rigid polyurethane foams, a dispersion time of 2 min was fixed for all nanofillers. This first step was carried out on a bath of ice and water to avoid temperature rise during sonication. Then, cyclopentane was added to the polyol/nanofiller suspension which was stirred at 2000 rpm for 30 s using a mechanical stirrer (IKA-WERKE/ Eurostar-Power B) based on the literature.[6,11,13,26] Finally, the isocyanate was added to the mixture which was additionally mixed for 5 s. Then, the mixture was poured into an open rectangular aluminum mold (Figure 3) (length = 20 cm, width = 10 cm, thickness = 4 cm) designed for this study. All the foams were analyzed after a curing time of 24 h. The formulation used for the foams preparation was given in Table II.

Characterization Methods

To study the effect of the types and shapes of nanofillers on the rheological behavior of the different polyol/nanofiller suspensions, rheological measurements were performed. These measurements were carried out using a Malvern/Bohlin Gemini 200 Rheometer and a plate-plate geometry with grooved plates in order to avoid a slippage. The gap was fixed at 150 μm and frequency sweep test measurements were performed from 0.1 to 100 rad s^{-1}, with a constant stress of 40 Pa at 25 °C. As mentioned above, to obtain a homogeneous dispersion of the nanofillers in polyol, the mixtures were sonicated for 2 min with an ultrasonic homogenizer. The measurements were performed for polyol/nanofiller suspensions with different concentrations of

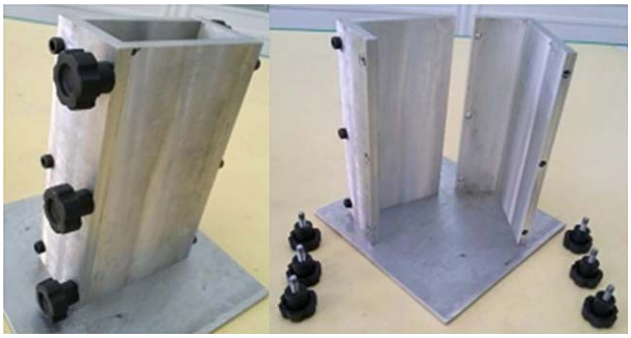

Figure 3. Rectangular mold designed for this study (length = 20 cm, width = 10 cm, thickness = 4 cm). [Color figure can be viewed in the online issue, which is available at wileyonlinelibrary.com.]

Table II. Formulation of Neat and Nanofilled Rigid Polyurethane Foams

Materials	Materials content (wt %)		
Nanofiller	0	1.0	10.0
Polyol	38	37.6	34.2
Isocyanate	57	56.5	51.3
Cyclopentane	5	4.9	4.5

nanofillers to determine the percolation threshold. In addition, the viscosity of the suspensions was monitored.

The foaming reaction kinetics were monitored using an FTIR spectrometer (Bruker Tensor 27) fitted with a transmission accessory within a range of 400–4000 cm^{-1}. For these analyses, polyol/nanofiller/cyclopentane mixtures with 1 and 10 wt % of nanofillers were prepared followed by the addition of isocyanate. Immediately after the isocyanate was mixed with the polyol/nanofiller/cyclopentane mixture, a droplet of the reactive blend was placed on a pressure molded potassium bromide (KBr) pellet and FTIR spectrometry measurements were performed at a resolution of 4 cm^{-1} with a number of sample scans of 16 scans/spectrum. The reaction was monitored during 60 min with a scanning time per spectrum of 2 min. For each measurement, a background file was obtained for a neat KBr pellet at 4 cm^{-1} resolution with a number of sample scans of 16 scans/spectrum to eliminate the scattering phenomenon often observed in measurements with KBr pellets. The reaction kinetics study was conducted by monitoring the isocyanate absorbance decrease as a function of time. The evolution of isocyanate absorbance band obtained at different reaction times in the case of an unfilled rigid polyurethane foam is presented in Figure 4.

To correct the density change of the system, the integrated isocyanate absorbance was normalized by the integrated absorbance of an internal reference which remained constant during the reaction.[26] In this study, the CH stretching region (2960 cm^{-1}) was chosen as the reference band. Then, to study the foaming reaction kinetics, the isocyanate conversion (ρ_{NCO}) was calculated using eq. (1). A_t and A_0 represent the normalized absorbance values at a time t and at zero reaction time, respectively.

$$\rho_{NCO} = 1 - \frac{A_t}{A_0} \quad (1)$$

The structure of the foams was examined with a scanning electron microscope (SEM) at 20 kV. A gold/palladium coating was applied on all samples before the morphological characterization. The location of the analyzed samples into the rigid polyurethane foam is presented in Figure 5. SEM images were obtained for parallel and perpendicular foam sections to the foaming direction.

Cell size measurements were carried out from SEM images using Image J software. To evaluate the effect of nanofillers on foams, an average cell diameter was determined from at least 80 cells using SEM images of perpendicular sections to the foaming direction for each sample.

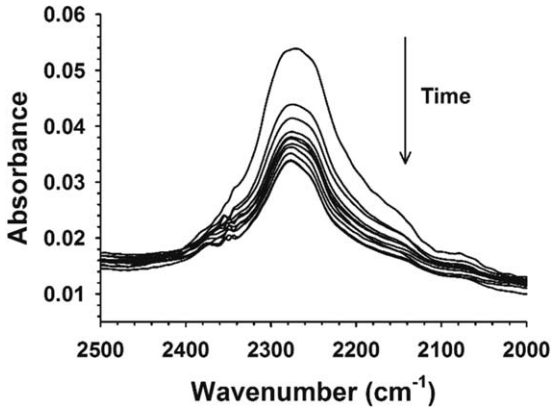

Figure 4. Infrared spectra of an unfilled rigid polyurethane foam sample obtained at different reaction times from 0 to 60 min, every 30 s for the first 7 spectra and every 15 min for the last five spectra.

RESULTS AND DISCUSSION

Effects of Nanofillers Type and Shape on Rheological Percolation Threshold of the Polyol/Nanofiller Suspensions

The understanding of rheological properties of polymer/nanofiller nanocomposites is important to optimize their preparation. The results of linear viscoelasticity measurements performed for the different polyol/nanofiller suspensions are presented in Figure 6. At low frequencies, until a certain amount of nanofiller content is reached, an increase of the elastic modulus is observed and the system exhibits a liquid-like behavior. As mentioned in Experimental section, we assumed that a homogenization time of 2 min allowed a good dispersion of the nanofillers in polyol. Thus, we can suppose that the dispersion is good until the percolation threshold is attained. From this value and above, the elastic modulus (G') reaches a plateau, which is characteristic of a solid-like material and a network of nanofillers is formed in the polymeric matrix. At high frequencies, the effect of the polymer matrix on G' is more important than the effect of nanofillers, and an increase of the nanofillers amount induces an increase of the elastic modulus. This evolution can be explained with an increase of the deformation rate in the matrix. In the literature, various methods are used to assess the percolation threshold.[20–22,34]

In this study, the rheological percolation threshold was determined by plotting the elastic modulus measured at the lowest accessible frequency (which was obtained from the graphs in Figure 6 for each suspension) as a function of the volume fraction of nanofillers (Figure 7). Figure 7 shows that, for low volume fractions of nanofillers (φ), the elastic modulus is low and

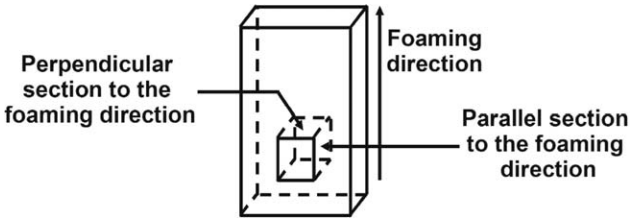

Figure 5. Location of polyurethane foam samples used for morphological analysis.

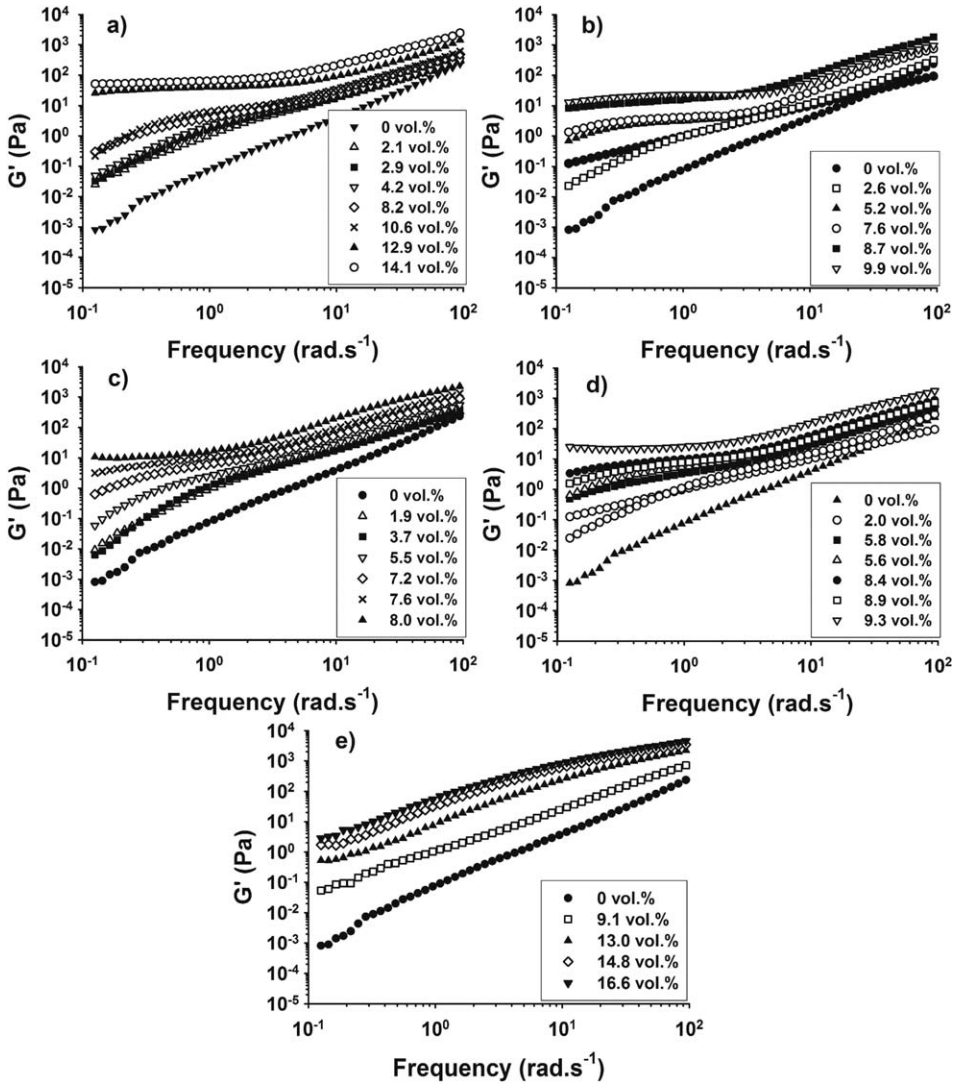

Figure 6. Evolution of the elastic (G') modulus for different polyol/nanofiller systems containing: (a) TiO_2 nanospheres, (b) TiO_2 nanorods, (c) ZnO nanospheres, (d) ZnO nanoplatelets, and (e) Fe_3O_4 nanoplatelets.

seems independent of φ. Above a critical value of the volume fraction, G' increases sharply as described in the literature.[22,23,34] For each suspension, the volume fraction at percolation (φ_c) can then be estimated from the intersection of the two regions in the graphs in Figure 7. Rheological percolation thresholds (φ_c) obtained for the different polyol/nanofiller suspensions are presented in Table III.

The effect of the nanoparticles shape on φ_c was considered through the aspect ratio comparing results obtained for TiO_2 or ZnO nanospheres with those determined for their respective nanorods or nanoplatelets. In the case of TiO_2, a higher percolation threshold was observed for nanospheres ($\varphi_c = 10.7$ vol %) compared to nanorods ($\varphi_c = 7.2$ vol %). However, for ZnO nanospheres ($\varphi_c = 7.2$ vol %) and nanoplatelets ($\varphi_c = 8.5$ vol %), the latter conclusion is reversed and a smaller difference between the two nanofillers was observed. The percolation threshold of polymer/nanofiller suspensions depends on the nanoparticles dispersion state but also on the nanofiller shape and dimensions.[21,34–36] Experimental and theoretical studies have shown that the effect of the aspect ratio of nanoplatelets or short carbon fibers on the percolation threshold was predominant.[21,34–36] A lower percolation threshold was observed for nanoparticles compared to microscaled fillers which was explained by the higher aspect ratio and the large surface area of nanoparticles. Li *et al.*[21] studied polymer/carbon nanotubes (CNTs) systems and showed that the percolation threshold decreased linearly, ultimately reaching a plateau as the aspect ratio increased. They also showed that for aspect ratios above a critical value, the percolation threshold became almost constant and independent of the aspect ratio, depending only on the dispersion parameters. In our study, the evolution of the percolation threshold of TiO_2 nanospheres and nanorods is in correlation with the literature. For ZnO nanoparticles, the small increase of the percolation threshold as the aspect ratio increases can be explained by the lower specific surface area of ZnO nanoplatelets compared to nanospheres (Table III) despite their higher aspect ratio.

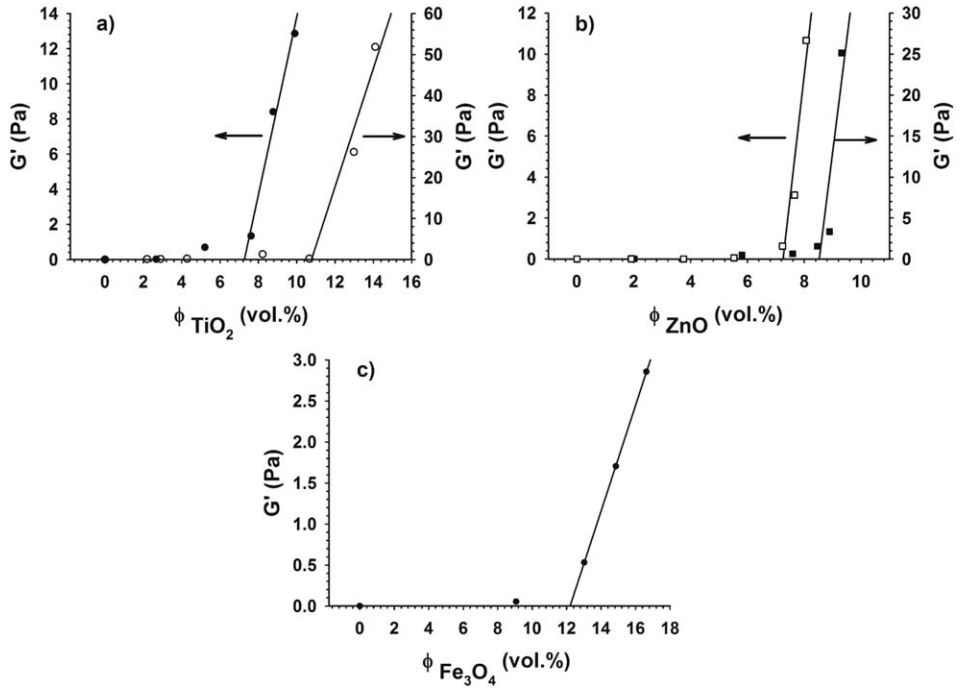

Figure 7. Elastic modulus (G') vs. volume fraction of nanofillers (φ) for the different polyol/nanofiller systems: (a) TiO_2 nanospheres (○) and nanorods (•), (b) ZnO nanospheres (□) and nanoplatelets (■), and (c) Fe_3O_4 nanoplatelets (•).

The effect of nanoparticles type on the percolation threshold was also investigated. The comparison of results obtained for suspensions containing TiO_2 nanospheres and ZnO nanospheres shows that the percolation threshold is higher for the polyol/TiO_2 nanospheres suspension. It should also be noticed that the specific surface area of TiO_2 nanospheres is higher than that of ZnO nanospheres, even though their aspect ratio is the same, which seems to induce a higher percolation threshold.

The comparison of suspensions containing ZnO nanoplatelets and Fe_3O_4 nanoplatelets according to the specific surface areas shows the same tendency. However, these nanoparticles do not have the same aspect ratio. Li *et al.*[22] studied the percolation threshold of conducting polymer/disc-shaped composites and developed an analytical model in correlation with their experimental results, allowing the prediction of this threshold. For a given thickness of nanofillers, the percolation threshold decreased with an increase of the nanofillers diameter. In this study, in the case of the suspensions with ZnO nanoplatelets, Fe_3O_4 nanoplatelets, and TiO_2 nanorods (assuming an approximation as they have one dimension higher than the others), when the aspect ratio increased, a decrease of the percolation threshold was observed, independently of the nanofillers type. These results are in correlation with those obtained in the literature for graphite nanoplatelets.[22] Therefore, a predominant effect of the aspect ratio of nanofillers on the rheological percolation threshold can be noticed compared to the nanofillers type.

Effects of the Type, Shape, Concentration, and Surface Area of the Nanofillers on the Foaming Reaction Kinetics

The type, shape, and surface area effects of TiO_2 nanospheres and nanorods, ZnO nanospheres and nanoplatelets, and Fe_3O_4 nanoplatelets on the foaming reaction kinetics were studied by comparing the conversion curves of mixtures with nanofiller

Table III. Percolation Thresholds (φ_c) of the Different Polyol/Nanofiller Systems

Polyol/nanofiller suspensions	φ_c (vol %)	Diameter/length (nm)	Thickness (nm)[b]	Aspect ratio[b]	Specific surface area[c] ($m^2\ g^{-1}$)
Polyol/TiO_2 nanospheres	10.7	<25[a]	-	1	39.3
Polyol/TiO_2 nanorods	7.2	3701[b]	62	59.7	51.3
Polyol/ZnO nanospheres	7.2	25-30[a]	-	1	31.6
Polyol/ZnO nanoplatelets	8.5	1423[b]	50	28.4	19.9
Polyol/Fe_3O_4 nanoplatelets	12.2	320[b]	35	9.1	32.3

The diameter, thickness, aspect ratio, and specific surface area of the corresponding nanoparticles are also given.
[a] Suppliers' values.
[b] SEM.
[c] BET.

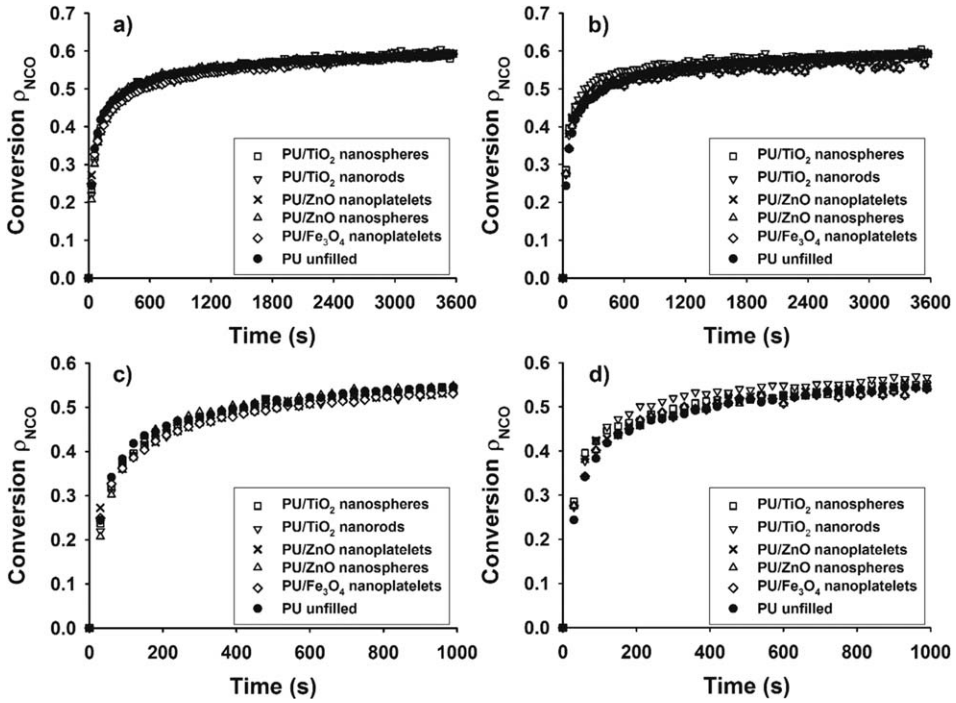

Figure 8. The isocyanate conversion of polyurethane/nanofiller systems with respect to time for different concentration of nanofiller in polyol: (a) 1 wt % and (b) 10 wt %. (c) and (d) represent the first 1000 s of the reaction for 1 and 10 wt %, respectively.

contents of 1 and 10 wt % in polyol (Figure 8). For both concentrations and each type of nanofiller, the corresponding volume fraction in polyol is given in Table IV. These concentrations were purposely chosen below the rheological percolation threshold (Table III) for each system. In Figure 8, when the concentration increases from 1 to 10 wt %, a more significant effect of nanofillers on the reaction kinetics can be noticed with a more visible effect at the initial stage of the reaction. To have a better understanding of nanofillers impact, the isocyanate conversion rate (k) of the different foaming reactions were determined from the graphs presented in Figure 8. According to conversion curves, we assumed that most of the isocyanate groups were consumed during the first 90 s. In this time range, the curves seem linear and they pass through the origin. Thus, the isocyanate conversion rate was determined from the slope. The results are presented in Table IV.

These results show that, for the lowest concentration (1 wt % in polyol), the conversion rate exhibits a slight variation compared to the unfilled foam for all nanofilled systems. Bernal *et al.*[26] obtained similar results for polyurethane/carbon

Table IV. Isocyanate Conversion Rates (k) and Zero Shear Viscosities (η_0) Obtained for Polyurethane/Nanofiller Systems

	[Nanofiller] (wt %)							
	1	10	1	10	1	10		
PU/Nanofiller systems	$\varphi_{nanofiller}$[a] (vol %)		$k \times 10^3$ (s^{-1})[b]		η_0 (Pa s)[c]		Nanofillers aspect ratio[d]	Nanofillers-specific surface area ($m^2\ g^{-1}$)[e]
PU/Unfilled			4.61		12.5		-	0
PU/TiO_2 nanospheres	0.29	2.9	4.75	5.44	13.4	26.5	1	39.3
PU/TiO_2 nanorods	0.27	2.7	4.56	5.48	15.3	28.1	59.7	51.3
PU/ZnO nanospheres	0.19	1.9	4.48	5.21	14.2	21.6	1	31.6
PU/ZnO nanoplatelets	0.20	2.0	4.73	5.05	14.4	18.9	28.4	19.9
PU/Fe_3O_4 nanoplatelets	0.25	2.5	4.70	5.15	14.4	24.2	9.1	32.3

Volume fractions, aspect ratios, and specific surface areas of nanofillers are also given.
[a] Volume fraction of nanofiller in polyol.
[b] FTIR.
[c] Rheological measurements.
[d] SEM.
[e] BET.

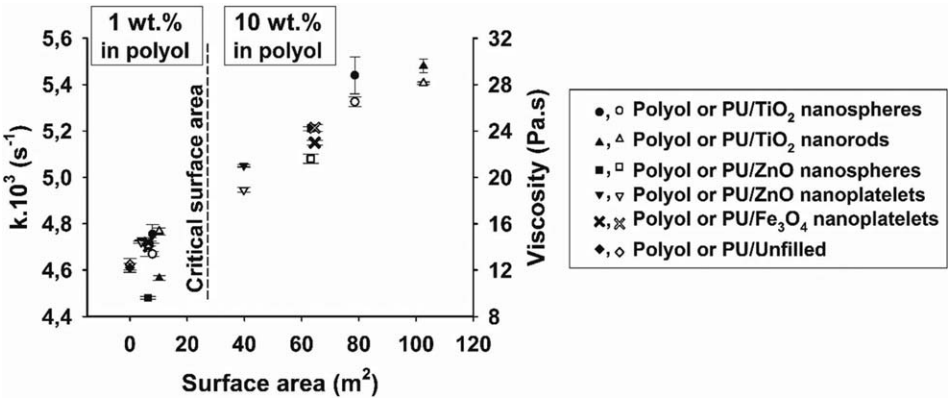

Figure 9. Evolution of the conversion rate (filled symbols) for the PU/nanofiller systems and the viscosity (unfilled symbols) for polyol/nanofiller suspensions as a function of the surface area of the whole nanofillers introduced in the systems.

nanotube systems (0.3 wt %) with a lower conversion rate than the unfilled sample, also at the early stages of the reaction. They particularly showed that the isocyanate conversion was dominated by the concentration of nanofillers rather than their functionality. Thus, for low concentrations of nanoparticles, nanofillers, as well as their type and their shape have no effect on reaction kinetics. Therefore, it can be concluded that, for low concentrations, the chemical reaction mainly depends on the viscosity of the reacting medium of nanofilled foams (between 13.4 and 15.3 Pa s) which is higher than the viscosity of the neat polyurethane foam (12.5 Pa s). This leads to a lower mobility of the reacting chains in the system and, in some cases, to a lower conversion rate (PU/TiO_2 nanorods and PU/ZnO nanospheres systems). This conclusion was mentioned by several authors to explain the evolution of the foaming process for polyurethane/carbon nanotubes[26,36] and silicone/carbon nanotubes or graphene[37] systems. Concerning the highest nanofiller concentration (10 wt %), for all systems, the conversion rate increased compared to the unfilled foam and to the foams prepared at 1 wt %. These results imply that the conversion rate increases when a critical amount of nanofillers is reached and above this critical concentration, the nanofillers probably act as catalysts for the reaction. This behavior was already observed for polyurethane foam/clay nanocomposites[30] with a filler content of 3 wt % and for polyurethane/clay nanocomposites[27] with a filler concentration of 5 and 10 wt %. Furthermore, as expected, zero shear viscosities (η_0) measured for the suspensions prepared at 10 wt % were higher than those obtained for suspensions at 1 wt %. Besides, these results exhibit a more significant variation between the nanofiller types and shapes compared to foams at 1 wt %. For the highest concentration of nanofiller (10 wt %), the comparison of the systems containing TiO_2 and ZnO nanospheres with those of their respective nanorods and nanoplatelets, shows that the isocyanate conversion rates follow the same trend as the viscosities. The conversion rate and viscosity are lower for PU/TiO_2 nanospheres system with respect to PU/TiO_2 nanorods system. However, for ZnO nanoparticles, the conclusions are reversed. Assuming that all the materials used in this study and the effects of impurities throughout these materials were uniform, this result can be attributed to the lower specific surface area of ZnO nanoplatelets compared to ZnO nanospheres (Table IV). Furthermore, for foams containing TiO_2 nanorods, ZnO nanoplatelets, and Fe_3O_4 nanoplatelets, when the specific surface area of the nanofillers increased, the viscosity as well as the conversion rate increased. Although it seems difficult to draw comparisons between the nanofiller types, these results indicate a significant effect of the nanofillers shape rather than their type on the conversion rate of the reaction, for high concentrations of nanofiller (10 wt %).

Figure 9 represents the viscosity and the conversion rate as a function of the surface area of the whole nanofillers introduced in the system. The latter was calculated using the specific surface area and the weight of nanofillers introduced at 1 and 10 wt % in polyol. This figure brings out two different behaviors. For low surface areas, the conversion rate remains rather constant although a slight increase of the viscosity is observed as the surface area increases. For higher surface areas and more precisely above a critical value, the effect of the surface area on reaction kinetics becomes more significant, and hence the conversion rate increases as the surface area rises, despite an important increase of the viscosity of the reacting medium which reduces the mobility of the molecules. In the literature, Wilkinson *et al.*[27] studied PU/nanoclay systems and explained the rise of the reaction rate as the nanofiller concentration increased by the presence of water between the nanoclay. However, in this study, since only oxide nanofillers were used such significant effect of water would not be expected. As a result, for high surface areas, nanofillers act as catalyst for the reaction. Subsequently, up to 18% (±3%) faster reactions were observed compared to the unfilled polyurethane foam in the TiO_2 nanorods containing PU system. The calculations were based on the comparison of the isocyanate conversion rates obtained for the neat and nanofilled polyurethane foams (Table IV and Figure 9).

Effects of the Type, Shape, and Concentration of the Nanofillers on the Microstructure Development

SEM images of the foam samples are presented in Figure 10. The measurements were performed for parallel and perpendicular foam sections to the foaming direction. In the first case (parallel sections), the foam cells are elongated in the foaming direction for all systems. Thus, only the image of the unfilled

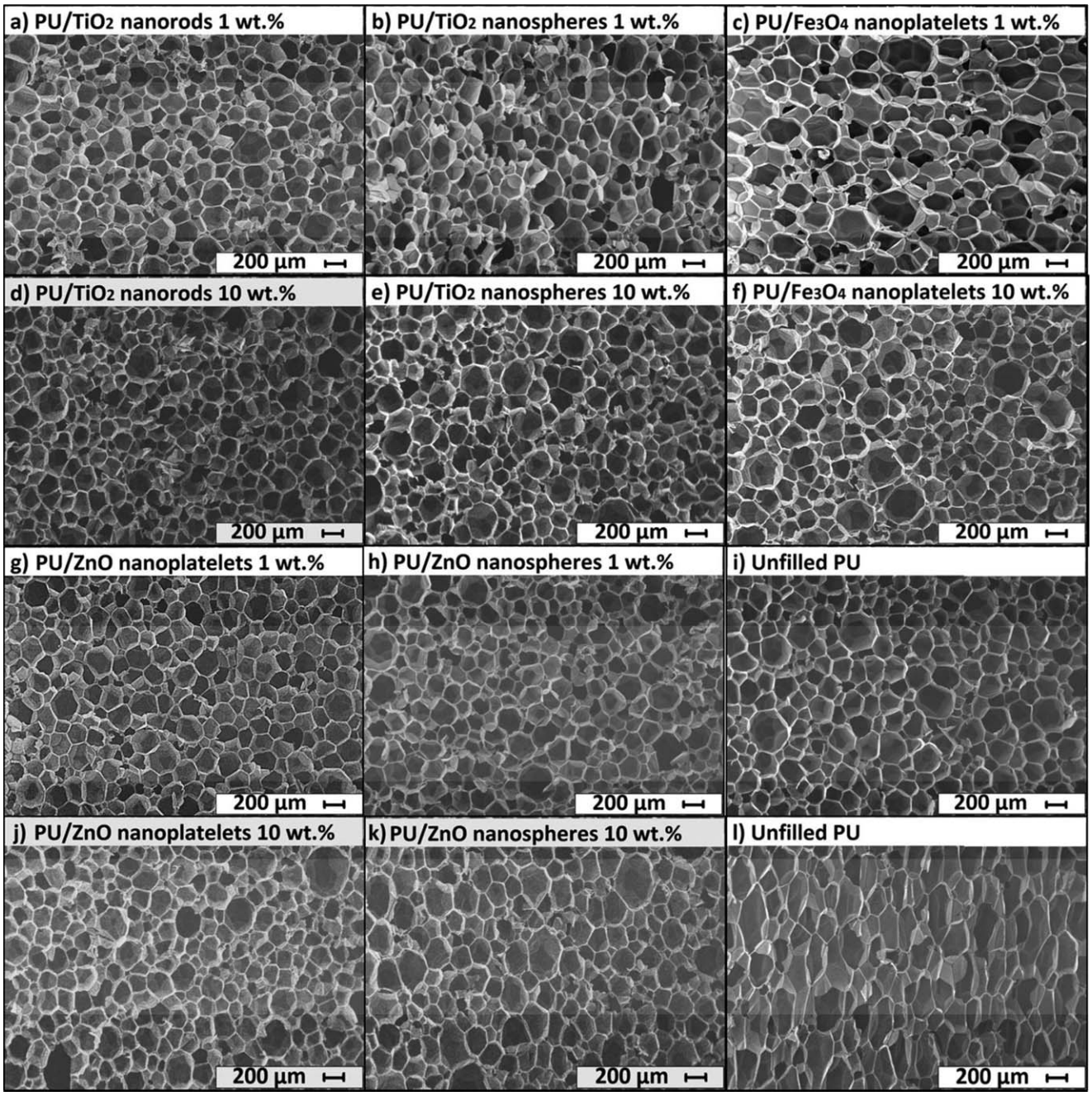

Figure 10. SEM images of PU/nanofiller systems obtained for concentrations of nanofiller of 1 wt % (a,b,c,g,h) and 10 wt % (d,e,f,j,k) in polyol for perpendicular (all cases except l) and parallel (l) foam sections to the foaming direction (accelerating voltage: 20 kV; magnification: 100×).

foam is presented here (Figure 10, image l). In the second case (perpendicular sections), the cellular section seems isotropic.

Cell diameter distributions (as d_{50} and d_{90}; d_{50} and d_{90} refer to 50 and 90% of the cells below a particular size, respectively) of the foams were determined from images of perpendicular section to the foaming direction as described in Experimental Section using Image J software. The results are gathered in Table V.

For both concentrations and all nanofilled foams, a decrease of the cell diameter up to 40% (compared to the unfilled foam) was observed for the nanofilled systems compared to the unfilled one. This drop was much more significant for foams with a nanofiller concentration of 10 wt % in polyol. For example, while the cell diameter distribution d_{90} for 1 wt % ZnO nanospheres containing system was 200 μm, it was reduced to 160 μm when 10 wt % of nanofiller was added to the system. That means cell size was reduced by 20% when nanofiller content was changed from 1 to 10 wt %. Therefore, the addition of nanofillers resulted in foams with smaller cells. In the literature, the decrease of the cell size in polyurethane/nanoclay[18,38] and polystyrene/carbon nanofiber[39,40] systems was explained by an increase of the cell density induced by a significant increase of

Table V. Cell Diameters (d_{50} and d_{90}) Obtained for Polyurethane/Nanofiller Systems

	[Nanofiller] (wt %)			
	Cell diameter, d_{50} (μm)[a]		Cell diameter, d_{90} (μm)[a]	
PU/Nanofiller systems	1	10	1	10
PU/Unfilled	227		236	
PU/TiO_2 nanospheres	208	181	200	180
PU/TiO_2 nanorods	175	145	179	141
PU/ZnO nanospheres	191	164	200	160
PU/ZnO nanoplatelets	200	145	188	155
PU/Fe_3O_4 nanoplatelets	220	168	208	167

[a] SEM.

nucleation sites due to the presence of the nanofillers. In our study, as the nanofillers were dispersed in the polyol and considering that the dispersion was good as demonstrated in the Experimental Section ("Foam preparation" part), we assumed that the viscosity of the PU/nanofiller system corresponded to the viscosity of the polyol/nanofiller suspension. Therefore, the zero shear viscosities obtained for the different polyol/nanofiller suspensions (1 and 10 wt %) can represent the viscosities of the reacting systems and the cell size variations can be related to the viscosity of the PU/nanofiller systems. The results are gathered in the Table VI and, as expected, they show a higher viscosity for all suspensions compared to the unfilled foam and an increase of the suspension viscosity as the nanofiller concentration increases from 1 to 10 wt %. As a result, we can conclude that the cell diameter decreases due to the increase in viscosity of the reacting medium and possible presence of higher number of nuclei.

The effect of the nanofillers shape on the morphology of the foam was also investigated. Thus, the effect of the nanofillers aspect ratio was studied comparing foams filled with TiO_2 and ZnO nanospheres to those containing their respective nanorods and nanoplatelets. Although the specific surface area of TiO_2 nanospheres was smaller than that of TiO_2 nanorods and the specific surface area of ZnO nanospheres was greater than that of ZnO nanoplatelets, the cell sizes obtained for foams filled with nanospheres were larger compared to foams filled with nanorods and nanoplatelets. For foams with TiO_2 nanorods, a smaller cell size compared to the foams containing TiO_2 nanospheres was observed. The same tendency was observed for ZnO nanospheres and nanorods. This evolution of cell size can be explained by the flat surfaces of TiO_2 nanorods and ZnO nanoplatelets, allowing a more notable effect of these nanoparticles on the cell nucleation process. Consequently, more nucleation sites were formed with these nanoparticles. This induced the formation of smaller cells compared to the foams containing nanospheres. Furthermore, as the viscosity of the reacting medium was higher in the case of TiO_2 nanorods, less expanded foams were obtained. However, the reversed conclusion about the viscosities for ZnO nanoparticles underlines the less important effect of the viscosity on the final foam structure. As a result, the flat surfaces of nanorods and nanoplatelets allowing an increase of the number of the nucleation sites induce a reduction of the cell sizes.

The effect of the nanoparticles type on the foam morphology was also considered. No trend emerges from results obtained for systems filled with nanospheres. Therefore, comparison between foams containing TiO_2 nanorods, ZnO, and Fe_3O_4 nanoplatelets shows a decrease of the cell size as the aspect ratio increases, independent of the nanofiller type. This result emphasizes a predominant effect of the nanofiller shape on the cell size rather than its type as observed above for reaction kinetics results. The close values of the thicknesses of nanoplatelets (Table I) allow to conclude that the mean cell size decreases with an increase of the nanoplatelets aspect ratio. Thus, this study shows a predominant effect of the aspect ratio of nanofillers on microstructure development rather than their type. It should also be noticed that, in addition to their shape, the

Table VI. Cell Diameters and Zero Shear Viscosities (η_0) Obtained for Polyurethane/Nanofiller Systems

	[Nanofiller] (wt %)					
	Cell diameter, d_{90} (μm)[a]		η_0 (Pa s)[b]			
PU/Nanofiller systems	1	10	1	10	Nanofillers aspect ratio[a]	Nanofillers-specific surface area ($m^2\ g^{-1}$)[c]
PU/unfilled	236		12.5		-	0
PU/TiO_2 nanospheres	200	180	13.4	26.5	1	39.3
PU/TiO_2 nanorods	179	141	15.3	28.1	59.7	51.3
PU/ZnO nanospheres	200	160	14.2	21.6	1	31.6
PU/ZnO nanoplatelets	188	155	14.4	18.9	28.4	19.9
PU/Fe_3O_4 nanoplatelets	208	167	14.4	24.2	9.1	32.3

Aspect ratios and specific surface areas of nanofillers are also given.
[a] SEM.
[b] Rheological measurements.
[c] BET.

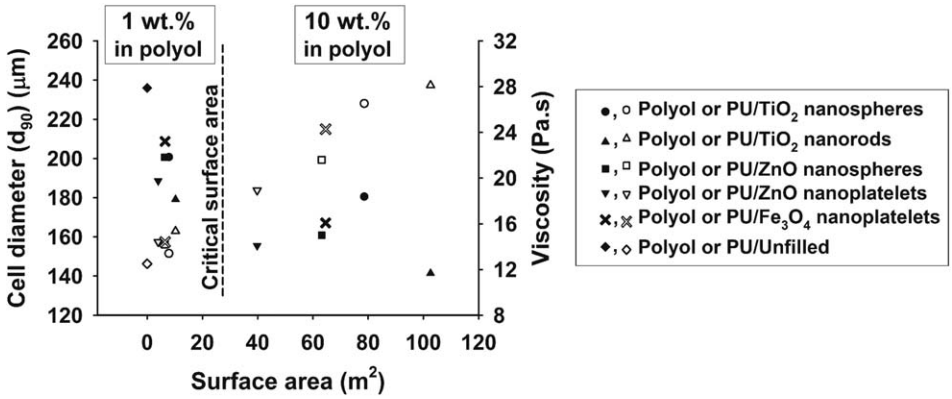

Figure 11. Evolution of the cell diameter (filled symbols) for the PU/nanofiller systems and the viscosity (unfilled symbols) for the polyol/nanofiller suspensions, as a function of the surface area of the whole nanofillers introduced in the systems.

surface features of the nanoparticles (flat) have obvious effects on microstructure development as the cell sizes were smaller for foams containing nanorods or nanoplatelets compared to those filled with nanospheres.

The effect of the nanoparticles concentration on the foams microstructure was also investigated. Thus, to thoroughly address the issue, the nanofillers concentration effect was studied through the surface area of the whole nanofillers in the foam. The latter was calculated as mentioned above, using the specific surface area of the nanofillers and their weight. Figure 11 shows the influence of the surface area on the viscosity and on the cell size of the foams.

Two different behaviors emerge as for the conversion rate evolution presented in Figure 9. For small surface areas which correspond to nanofiller concentration of 1 wt %, a sharp decrease of the cell size coupled with a slight increase of the viscosity were observed as the surface area increases. For high surface areas (10 wt %), no trend emerges. However, it could be noticed that, for a same nanofiller, the cell size was reduced when the surface area increased. Concerning the viscosity, an increase was observed when the surface area increased and as mentioned, this evolution induced a decrease of cell sizes. A close analysis of the micrographs in Figure 10 shows that the cell size distribution is not uniform and as the nanofiller content increases, cell size distribution gets wider as shown in Figure 12. The same evolution of the cell size distribution was observed for all nanofilled foams. Thus, only the results obtained for PU/TiO_2 nanorods systems (1 and 10 wt %) are presented here.

As shown in Figure 12, as the TiO_2 nanorods content increases from 1 to 10 wt %, the cell size distribution becomes broader. These results suggest that nanofiller addition to PU systems do not only affect nucleation but also growth process. Although it is not simple to explain this effect, the schematic presented in

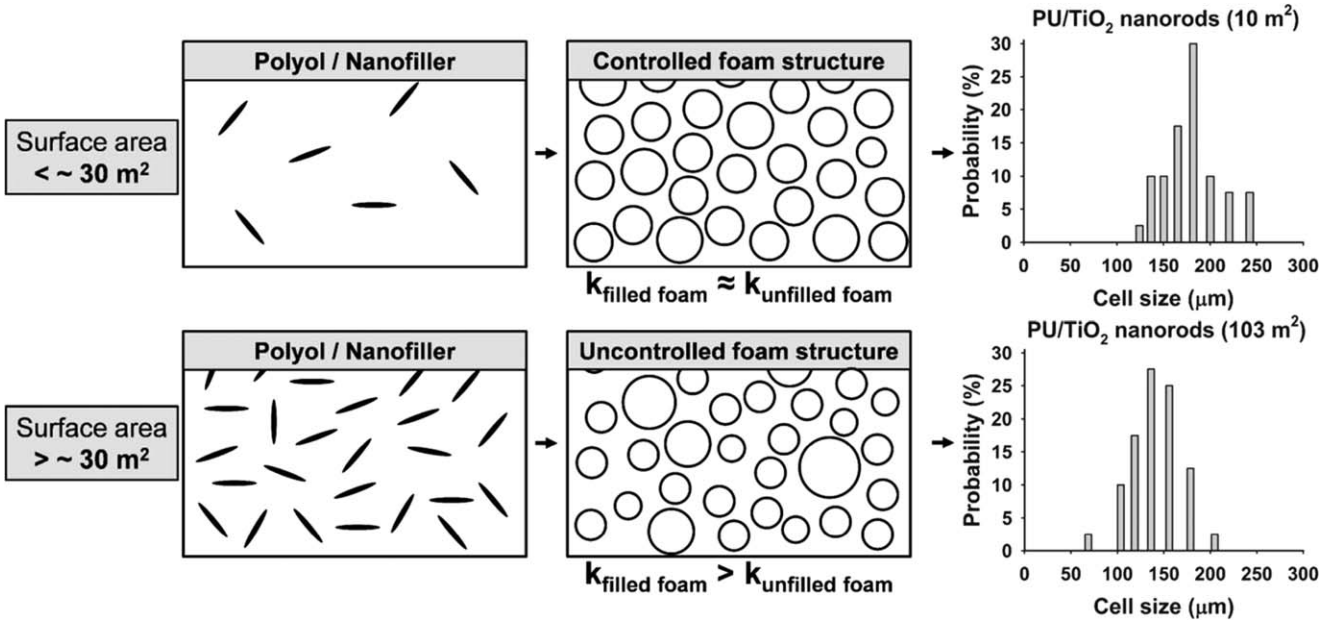

Figure 12. Effects of surface area and nanofiller concentration on isocyanate conversion rate and on final nanofilled rigid polyurethane foam morphology.

Figure 12 represents the role of nanofillers on final microstructure according to results in Figure 11 which demonstrate that, below a critical value, the narrower distribution of cell sizes allows the formation of a more controlled foam structure. These results show that, independently from nanofillers type, the introduction of oxide surfaces via nanofiller addition reduces final cell size up to a critical surface area (≈30 m^2). However, above this critical value, cell size distribution gets wider and the cell size can no longer be correlated with the surface area. Uncontrolled foam structure development can be attributed to faster exothermic polymerization reaction and hence uncontrolled cell nucleation, growth, and thus coalescence which results in an uncontrolled foam structure. Further research is still required to develop an understanding on this subject.

CONCLUSIONS

Properties of polyurethane rigid foams are mainly controlled by their microstructure which is influenced by the processing conditions. For tailoring microstructure of polyurethane foams, nanofillers are widely used. However, understanding their role, not only on the final microstructure but also on foam evolution, can enable researchers to better control the processing conditions to achieve desired microstructure and hence properties. Accordingly, in this study, a rheological investigation of polyol/nanofiller suspensions using various nanofillers with different types, shapes, and concentrations was performed. Reaction kinetics and microstructure analyses of the rigid polyurethane foam nanocomposites were also conducted. For foams containing TiO_2 nanorods, ZnO nanoplatelets, and Fe_3O_4 nanoplatelets, a decrease of the percolation threshold as the aspect ratio increased was observed. These results allowed to conclude that the effect of the nanofillers shape (through their aspect ratio and surface area) is predominant compared to their type. TiO_2 nanospheres containing suspensions presented a higher percolation threshold as compared to the suspensions containing TiO_2 nanorods. A less significant difference of percolation threshold was observed between suspensions with ZnO nanospheres and nanoplatelets, underlining again the importance of the shape effect of nanofillers. The polyurethane formation reaction kinetics were monitored *in situ* via isocyanate conversion. The results show that regardless of nanofiller type, there is a critical surface area, of nanofillers, (≈ 30 m^2 in this study) above which reaction kinetics increase as the surface area increases. The conversion rate increased up to 18% in presence of nanofillers with respect to unfilled foam. Below the critical surface area value, reaction kinetics were not affected by the surface area of nanofillers, suggesting that, to dominate the nucleation process in polyurethane rigid foam systems, there is a need to reach a critical surface area. Besides, independent of nanofillers type, the introduction of oxide surfaces via nanofiller addition reduces final cell size up to a critical surface area (≈ 30 m^2 in this study). However, above this critical value, cell size distribution gets wider and the cell size can no longer be correlated with the surface area. Uncontrolled foam structure development can be attributed to faster exothermic polymerization reaction and hence uncontrolled cell nucleation, growth, and hence coalescence. An important and interesting observation of this study is that all oxides used exhibit similar patterns of effects on viscosity, reaction kinetics, and cell size. This behavior suggests that in oxide nanofillers containing polyurethane rigid foams, the surface area of the nanofillers is a crucial parameter which can be used to tailor viscosity, reaction kinetics, and hence final microstructure. Moreover, the results of this study present a base for further studies in this area such as investigation of catalyst type effect on microstructure development and properties in nanofiller-added polyurethane foam systems.

ACKNOWLEDGMENTS

Burcu Ceren Dabak is acknowledged for the production of TiO_2 nanorods and ZnO nanoplatelets used in this study. The Scientific and Technological Research Council of Turkey (TUBITAK) and the Scientific Projects Commission of Anadolu University (under the contract number of 1404F169) are also gratefully acknowledged for their financial support.

REFERENCES

1. Wilkes, G. L.; Wildnauer, R. *J. Appl. Phys.* **1975**, *46*, 4148.
2. Datta, J. *J. Elastom. Plast.* **2010**, *42*, 117.
3. Klempner, D.; Sendijarevic, V.; Aseeva, R. M. Handbook of Polymeric Foams and Foam Technology; Hanser Gardener Publications: Munich, Cincinnati, **2004**.
4. Lee, L.; Zeng, C.; Cao, X.; Han, X.; Shen, J.; Xu, G. *Compos. Sci. Technol.* **2005**, *65*, 2344.
5. Saha, M.; Mahfuz, H.; Chakravarty, U.; Uddin, M.; Kabir, M.; Jeelani, S. *J. Mater. Sci. Eng. A* **2005**, *406*, 328.
6. Saha, M. C.; Kabir, M. E.; Jeelani, S. *J. Mater. Sci. Eng. A* **2008**, *479*, 213.
7. Chen, L.; Rende, D.; Schadler, L. S.; Ozisik, R. *J. Mater. Chem. A* **2013**, *1*, 3837.
8. Grunbauer, H. J. M.; Bicerano, J.; Clavel, P.; Daussin, R. D.; de Vos, H. A.; Elwell, M. J.; Kawabata, H.; Kramer, H.; Latham, D. D.; Martin, C. A.; Moore, S. E.; Obi, B. C.; Parenti, V.; Schrock, A. K.; van den Bosch, R. In Polymeric Foams: Mechanisms and Materials; Lee, S. T., Ramesh, N. S., Eds.; CRC Press: Boca Raton, FL, **2004**; ; Chapter 7, p 253.
9. Cao, X.; Lee, L. J.; Widya, T.; Macosko, C. W. *Polymer* **2005**, *46*, 775.
10. Dolomanova, V.; Rauhe, J. C. M.; Jensen, L. R.; Pyrz, R.; Timmons, A. B. *J. Cell Plast.* **2011**, *47*, 81.
11. Nayani, M.; Gunashekar, S.; Abu-Zahra, N. *Int. J. Polym. Sci.* **2013**, *2013*, 717895. DOI: 10.1155/2013/717895.
12. Alavi Nikje, M. M.; Bagheri Garmarudi, A.; Haghshenas, M.; Mazaheri, Z. In Nanotechnology in Construction 3, Proceedings of the NICOM3, Prague, Czech Republic **2009**, p 149.
13. Pardo-Alonso, S.; Solorzano, E.; Rodriguez-Perez, M. A. *Colloids Surf. A* **2013**, *438*, 119.
14. Widya, T.; Macosko, C. W. *J. Macromol. Sci. Part B: Phys.* **2005**, *44*, 897.
15. Wilkes, G. L.; Bagrodia, S.; Humphries, W.; Wildnauer, R. *J. Polym. Sci. Polym. Lett. Ed.* **1975**, *13*, 321.

16. Liu, S.; Duvigneau, J.; Julius Vancso, G. *Euro. Polym. J.* **2015**, *65*, 33.
17. Chaudhary, A.; Jayaraman, K. *Polym. Eng. Sci.* **2011**, *51*, 1749.
18. Harikrishnan, G.; Lindsay, C. I.; Arunagirinathan, M. A.; Macosko, C. W. *ACS Appl. Mater. Interfaces* **2009**, *1*, 1913.
19. Ibe, O. C. Elements of Random Walk and Diffusion Processes; Wiley: Hoboken, NJ, **2013**.
20. Penu, C.; Hu, G. H.; Fernandez, A.; Marchal, P.; Choplin, L. *Polym. Eng. Sci.* **2012**, *52*, 2173.
21. Li, J.; Ma, P. C.; Chow, W. S.; To, C. K.; Tang, B. Z.; Kim, J. K. *Adv. Funct. Mater.* **2007**, *17*, 3207.
22. Li, J.; Kim, J. K. *Compos. Sci. Technol.* **2007**, *67*, 2114.
23. Zhou, L.; Li, G.; An, T.; Li, Y. *Res. Chem. Intermed.* **2010**, *36*, 277.
24. Gong, Q.; Wu, J.; Gong, X.; Fanb, Y.; Xia, H. *RSC Adv.* **2013**, *3*, 3241.
25. Javni, I.; Zhang, W.; Karajkov, V.; Petrovic, Z. S. *J. Cell. Plast.* **2002**, *38*, 229.
26. Bernal, M. M.; Lopez-Manchado, M. A.; Verdejo, R. *Macromol. Chem. Phys.* **2011**, *212*, 971.
27. Wilkinson, A. N.; Fithriyah, N. H.; Standford, J. L.; Suckley, D. *Macromol. Symp.* **2007**, *256*, 65.
28. Heintz, A. M.; Duffy, D. J.; Nelson, C. M.; Hua, Y.; Hsu, S. L.; Suen, W.; Paul, C. W. *Macromolecules* **2005**, *38*, 9192.
29. Li, W.; Ryan, A. J.; Meier, I. K. *Macromolecules* **2002**, *35*, 6306.
30. Kim, D. S.; Kim, J. T.; Woo, W. B. *J. Appl. Polym. Sci.* **2005**, *96*, 1641.
31. Ozoğut, U. C. Master Thesis, Anadolu University, Turkey, **2013**.
32. Yakaboylu, G. A. Master Thesis, Anadolu University, Turkey, **2011**.
33. Karunaratne, V.; Priyadharshana, G.; Gunasekara, S.; Kottegoda, N.; Senaratne, A. United States, Pub. No. US2012/0056121A1, **2012**.
34. Vermant, J.; Ceccia, S.; Dolgovskij, M. K.; Maffettone, P. L.; Macosko, C. W. *J. Rheol.* **2007**, *51*, 429.
35. Celzard, A.; McRae, E.; Deleuze, C.; Dufor, M.; Furdin, G.; Mareche, J. F. *Phys. Rev. B* **1996**, *53*, 6209.
36. Verdejo, R.; Stampfli, R.; Alvarez-Lainez, M.; Mourad, S.; Rodriguez-Perez, M. A.; Bruhwiler, P. A.; Shaffer, M. *Compos. Sci. Technol.* **2009**, *69*, 1564.
37. Verdejo, R.; Saiz-Arroyo, C.; Carretero-Gonzalez, J.; Barroso-Bujans, F.; Rodriguez-Perez, M. A.; Lopez-Manchado, M. A. *Eur. Polym. J.* **2008**, *44*, 2790.
38. Pardo-Alonso, S.; Solorzano, E.; Estravis, S.; Rodriguez-Perez, M. A.; de Saja, J. A. *Soft Matter* **2012**, *8*, 11262.
39. Shen, J.; Zeng, C.; James Lee, L. *Polymer* **2005**, *46*, 5218.
40. Shen, J.; Han, X.; Lee, L. J. *J. Cell. Plast.* **2006**, *42*, 105.